Overview of the CMD-3 results at the VEPP-2000 e^+e^- collider *

G.V.Fedotovich[1,2], A.N.Amirkhanov[1,2], A.V.Anisenkov[1,2], V.M.Aulchenko[1,2], V.S.Banzarov[1], N.S.Bashtovoy[1], A.E.Bondar[1,2], A.V.Bragin[1], S.I.Eidelman[1,2], D.A.Epifanov[1], L.B.Epshteyn[1,2,3], A.L.Erofeev[1,2], S.E.Gayazov[1,2], A.A.Grebenuk[1,2], S.S.Gribanov[1,2], D.N.Grigoriev[1,4], F.V.Ignatov[1], V.L.Ivanov[1,2] S.V.Karpov[1], V.F.Kazanin[1,2], A.A.Korobov[1,2], O.A.Kovalenko[1,2], A.N.Kozyrev[1,2], E.A.Kozyrev[1,2], P.P.Krokovny[1,2], A.E.Kuzmenko[1,2], A.S.Kuzmin[1,2], I.B.Logashenko[1,2], P.A.Lukin[1,2], K.Yu.Mikhailov[1,2], V.S.Okhapkin[1], Yu.N.Pestov[1], A.S.Popov[1,2], G.P.Razuvaev[1,2], A.A.Ruban[1], N.M.Ryskulov[1], A.E.Ryzhenenkov[1,2], V.E.Shebalin[1], D.N.Shemyakin[1,2], B.A.Shwartz[1,2], A.L.Sibidanov[4], Yu.M.Shatunov[1], E.P.Solodov[1,2], V.M.Titov[1], A.A.Talyshev[1,2], A.I.Vorobiov[1], Yu.V.Yudin[1,2]

[1] Budker Institute of Nuclear Physics, Novosibirsk, 630090, Russia
[2] Novosibirsk State University, Novosibirsk, 630090, Russia
[3] Novosibirsk State Technical University, Novosibirsk, 630092, Russia
[4] University of Sydney, School of Physics, Falkiner High Energy Physics Department, Australia

Abstract: The CMD-3 detector has been taking data since December 2010 at the VEPP-2000 electron-positron collider. The collected data sample corresponds to about 60 inverse picobarn of integrated luminosity in the c.m. energy range from 0.32 up to 2 GeV. Preliminary results of the analysis of various hadronic cross sections, in particular, $e^+e^- \to \pi^+\pi^-$, $\pi^+\pi^-\pi^0$, K_LK_S, K^+K^-, $\eta\gamma$, $3(\pi^+\pi^-)$, $2(\pi^+\pi^-\pi^0)$, $K^+K^-\pi^+\pi^-$, $K^+K^-\eta$, $K^+K^-\pi^0$, $\eta\pi^+\pi^-$, $\omega\pi^+\pi^-$ and $\omega \to \pi^0e^+e^-$ are presented. The processes with multihadron final states have several intermediate states which must be taken into account to correctly describe the angular and invariant mass distributions as well as cross section energy dependence.

Key words: hadrons, signal/background separation, cross section

PACS: 13.40.Gp, 13.66.Bc, 13.66.Jn PACS

1 Introduction

The electron-positron collider VEPP-2000 [1] has been operating at Budker Institute of Nuclear Physics since December 2010. The collider is designed to provide luminosity up to $10^{32}\text{cm}^{-2}\text{s}^{-1}$ at the maximum center-of-mass energy $\sqrt{s} = 2$ GeV. Two detectors, CMD-3 [2] and SND [3], are installed in the two interaction regions. The CMD-3 detector has high detection efficiency, good energy and angular resolutions for charged particles as well as for photons. The integrated luminosity collected by each detector is about 60 pb^{-1}.

The precision data on the hadronic cross sections are required, in particular, to evaluate the anomalous magnetic moment (AMM) of muon, $a_\mu = (g-2)_\mu/2$. The VEPP-2000 energy range gives the major hadronic contribution to AMM, both to the hadronic vacuum polarization itself ($\sim 92\%$) and to its uncertainty [4].

The precision of luminosity measurement is a key ingredient in many experiments which study the hadronic cross sections at e^+e^- colliders. It is very important to have several well-known QED processes such as $e^+e^- \to e^+e^-$, $\mu^+\mu^-$, $\gamma\gamma$ in order to perform cross checks and control the systematic uncertainty in luminosity determination. The CLEO collaboration was the first one to show in practice how a combined analysis of the processes $e^+e^- \to e^+e^-$, $\mu^+\mu^-$ and $\gamma\gamma$ helped to achieve a 1% accuracy for the luminosity [5]. The preliminary results on the luminosity determination and analysis of various hadronic cross sections for many processes are presented.

2 CMD-3 detector

Cryogenic Magnetic Detector is a general-purpose detector shown in Fig. 1. Coordinates, angles and momenta of charged particles are measured by the cylindrical drift chamber (DC) wich has a hexagonal cell. The coordinate resolution in the r-ϕ plane is ~ 120 μ. The coordinate along the beam axis is measured by charge division technique with resolution ~ 2 mm. The momentum resolu-

Received 30 November 2015

∗ Supported in part by the Russian Science Foundation (project N 14-50-00080), by the Russian Foundation for Basic Research grants RFBR 13-02-00215-a, RFBR 13-02-01134-a, RFBR 14-02-00580-a, RFBR 14-02-31275-mol-a, RFBR 14-02-00047-a, RFBR 14-02-31478-mol-a, RFBR 14-02-91332, RFBR 15-02-0567

1) E-mail: fedotovich@inp.nsk.su

tion goes like $\sigma_p/p \sim 1 \div 5\%$. The cylindrical multiwire double layer proportional Z-chamber is mounted directly behind DC and provides z-coordinate determination of the track by measuring the analogous information from cathode strips with an accuracy of $\sim$ 0.5 mm. The signals coming from anode sectors are used for the first level trigger and have time jitter $\sim$ 5 ns.

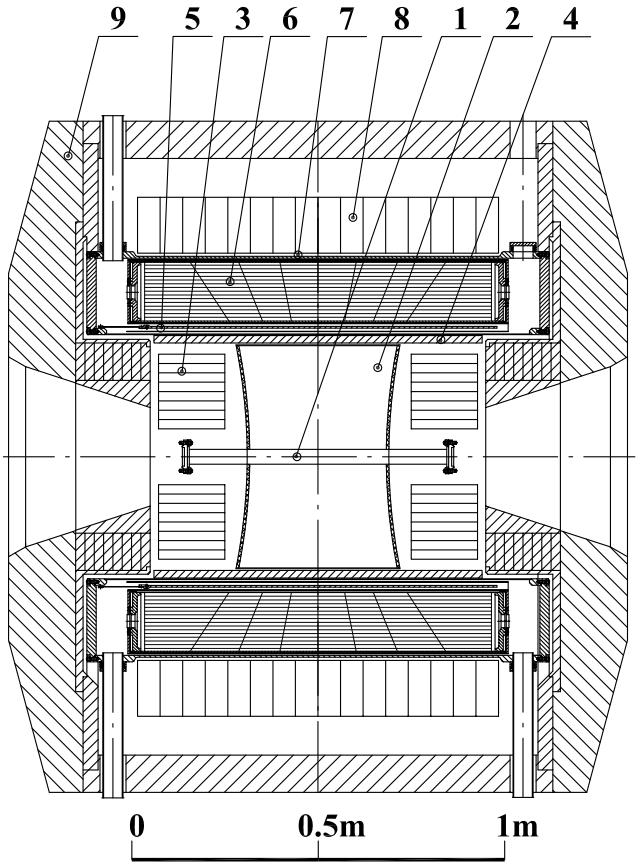

Fig. 1. CMD-3 detector: 1 – beam pipe, 2 – drift chamber, 3 – BGO, calorimeter, 4 – Z-chamber, 5 – SC solenoid, 6 – LXe calorimeter, 7 – TOF system, 8 – CsI electromagnetic calorimeter, 9 – yoke, not shown the outer muon range system.

The calorimeter of the detector consists of three parts. The endcap BGO calorimeter consists of 640 crystals with a thickness 13.4 X_0. The barrel part is placed outside of the $0.08X_0$ thin superconducting solenoid with 1.3 T magnetic field. The barrel calorimeter consists of two subsystems. The first one is based on Liquid Xenon calorimeter (5.4 X_0), the second one on the CsI crystals with the thickness 8.1 X_0 (1152 crystals) which are arranged in 8 octants. The LXe calorimeter has a tower structure (264 channels) and seven cylindrical double layers with strip readout (1286 channels). The strip information allows one to measure coordinates of the photon conversion point with precision $\sim 1 \div 2$ mm. The energy resolution of the barrel calorimeter was measured using Bhabha events and was found to be: σ_E/E $\sim 4 \div 8\%$.

The muon range system is mounted outside of the magnetic yoke and consists of 36 scintillation counters in the barrel part and 8 counters at the endcap. This system serves as the cosmic veto and has time resolution $\sim$ 1 ns.

3 Energy scan and luminosity measurement

The energy range from 1 to 2 GeV was scanned twice up and down with the step of 50 MeV in 2011 and in 2012. At each energy point the integrated luminosity $\sim$ 500 nb^{-1} was collected. The energy points during scan down (only in 2011) were shifted by 25 MeV with respect to the scan up. The beam energy was determined by measuring the momenta of Bhabha events with accuracy $\sim 1 \div 3$ MeV as well as using the Compton backscattering technique for several energy points near 2 GeV with accuracy $\sim$50 keV [6]. Two types of the first level triggers "CHARGED" and "NEUTRAL" were used while data taking. A special topological combination of signals from DC cells and Z-chamber, which roughly reproduce "track", start a special processor "TRACKFINDER" (TF). "CLUSTERFINDER" (CF) was started by signals coming from calorimeters. A positive decision of any trigger generates a command for the data acquisition system. The average trigger counting rate was about 200$\div$400 Hz while data taking.

The collected integrated luminosity is $\sim$60 pb^{-1} with about 34.5 pb^{-1} above the ϕ energy range, 8.3 and 8.4 pb^{-1} at the ω and ϕ resonances, respectively, and 9.4 pb^{-1} at low energies. The peak luminosity $\sim 2 \cdot 10^{31}$ cm^{-2}s^{-1} was reached and is currently limited by a positron injection rate. An upgrade of the injection facility will the gain of luminosity by a factor of ten is expected.

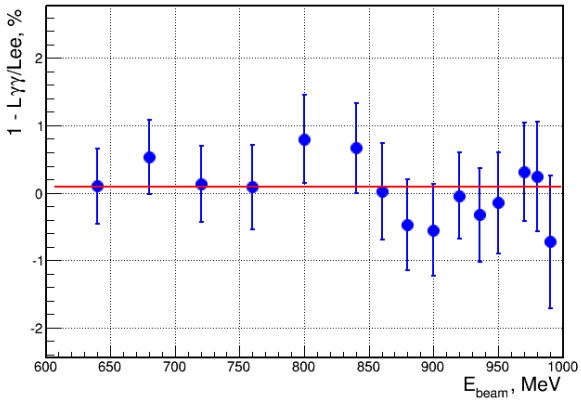

Fig. 2. The ratio of the relative difference of the luminosities vs beam energy (scan 2012).

The sample of collinear Bhabha events e^+e^- were selected for luminosity determination as well as the events of process $e^+e^- \to \gamma\gamma$ as an independent tool for cross check. The relative difference of the luminosities determined with two processes versus energy is presented in Fig. 2, where only statistical errors are shown (SCAN 2012) [7]. The horizontal line is a fit for this ratio and in average is about 0.2±0.3%. The main sources which contribute to systematic error are: interaction with material of the vacuum chamber wall $\sim$ (0.2÷0.4)%; the contribution due to the different angular resolution for Bhabha events and $\gamma\gamma$ is estimated as ∼0.8%; a correction which takes into account inclination of the beam axis with respect to the detector ∼0.4%, z-scale calibration accuracy of the DC wires contributes about 0.3 %. Presently we estimate the systematic accuracy as ∼1% for energies higher than 1 GeV.

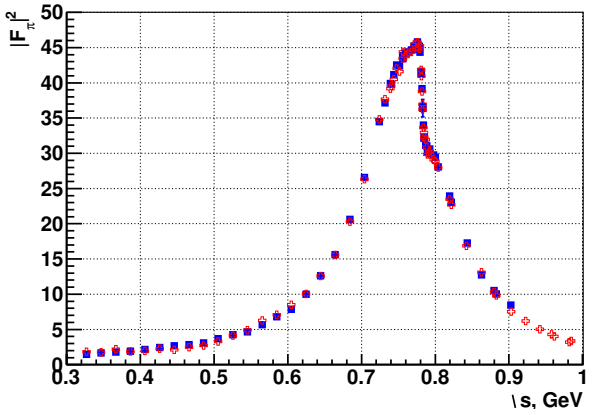

Fig. 3. Preliminary results of the pion form factor measurement. Squares - particle separation with momenta, points - particle separation with energy deposition in calorimeter

4 Pion form factor measurement

One of the main goals of the CMD-3 experiment is to reduce a systematic uncertainty of the cross section of two-pion production to the level smaller than 0.5%. In this case the uncertainty of the hadronic contribution to the AMM value, coming from this channel, will be 0.3÷0.4 ppm. The $\pi^+\pi^-$ events are separated either using the particle momenta or the energy deposition in the calorimeter. Two independent ways of event separation provide cross-check and allow to keep the systematic error under control.

Several features of the detector allow to reach the necessary level of systematic error. The fiducial volume is determined independently with the LXe calorimeter and the Z-chamber. The beam energy is measured with precision of $\sigma_E < 50$ keV using Compton backscattering of the laser light. The radiative corrections are calculated according to [8] with the accuracy better than 0.2%.

The first energy scan below 1 GeV was performed in 2013 [9]. The collected statistics is a few times higher than that in the previous CMD-2 measurements and it is at the level of ISR statistics collected by the BaBar and KLOE.

Preliminary results for the cross sections $\sigma(e^+e^- \to \pi^+\pi^-)$ measurements are shown in Fig. 3. The cross section of the process $e^+e^- \to \mu^+\mu^-$ was measured too. The results of the measurement are plotted in Fig. 4 with respect to the QED prediction and provide an important overall systematic test of the measurement. The horizontal line is a fit for the double ratio $(\sigma^{exp}_{\mu\mu}/\sigma^{QED}_{\mu\mu})/(\sigma^{exp}_{ee}/\sigma^{QED}_{ee})$ which was found to be (0.995±0.005)%.

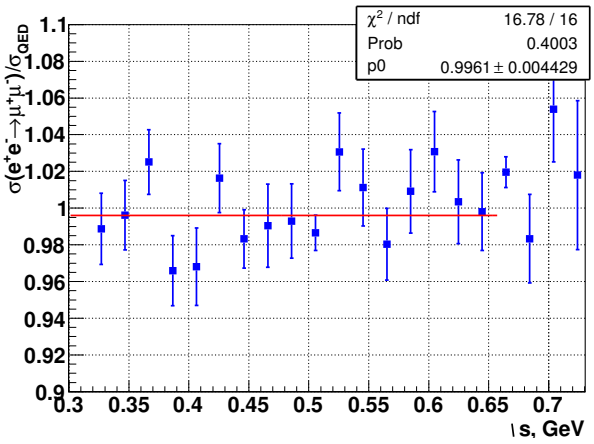

Fig. 4. Result of the measurement of muon pair production in comparison with the QED prediction.

5 Study of the processes $e^+e^- \to K_SK_L$ and $e^+e^- \to K^+K^-$

The most precise previous study of the process has been performed by the CMD-2 [10] and BaBar detectors. In this paper we present new measurement of the $e^+e^- \to K^0_SK^0_L$ and $e^+e^- \to K^-K^+$ cross sections. It is known the CMD-2 and BaBar results in the ϕ-peak region disagree at the level ∼5%, so new measurements are required. The $e^+e^- \to K^0_SK^0_L$ and $e^+e^- \to K^+K^-$ cross sections were measured in the c.m. energy range 1.004-1.060 GeV at 25 energy points. The detection of the neutral mode is based on the search of two central tracks with a common vertex in DC from the $K^0_S \to \pi^+\pi^-$ decay. Each track has momentum, that corresponds to the kinematically allowed region and has ionization losses of relativistic pions. The number of events is determined by

the fit of the two-pion invariant mass distribution with negligible background.

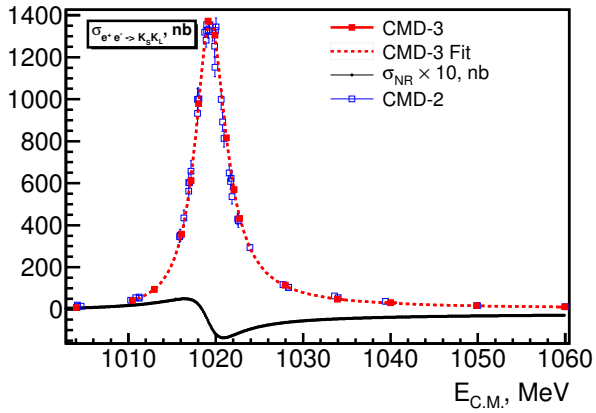

Fig. 5. The cross section of the process $e^+e^- \to K_L K_S$ around the ϕ-meson energy region. CMD-2, CMD-3 and BaBar data are presented. Black smooth curve (vertical scale increased by ten times) represents interference of the ϕ amplitude with ω, ρ and their excitations.

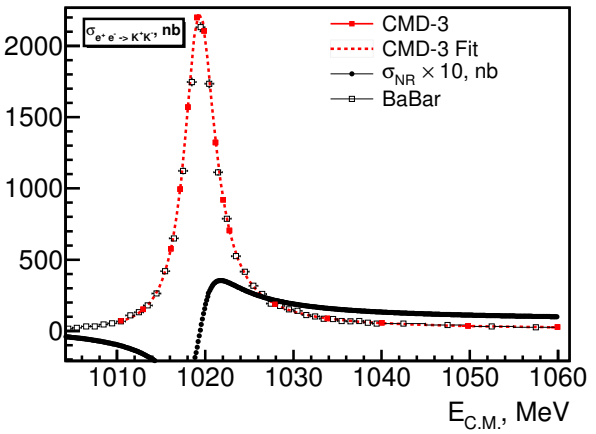

Fig. 6. The cross section of the process $e^+e^- \to K^+K^-$ around the ϕ-meson energy region. CMD-2, CMD-3 and BaBar data are presented. Black smooth curve (vertical scale increased by ten times) represents interference of the ϕ amplitude with ω, ρ and their excitations.

The detection of the charged mode is based on the search of two central collinear tracks of kaons with momentum known from DC. Each track has ionization losses significantly larger than m.i.p. due to relatively small velocity of kaons under study. After these requirements the level of remaining background is less than 0.5%. The detection efficiency of each kaon was determined with data as well as with MC simulation and delivers a deviation less 1.5%.

The obtained cross sections for neutral and charged mode together with the fit are presented in Fig. 5 and Fig. 6, respectively. Currently the systematic accuracy for these cross sections is estimated as 2% and 3%, respectively.

The measured cross section is approximated according to Vector Meson Dominance model as a sum of the ϕ, ω, ρ - like amplitudes and their excitations. The neutral and charged channels were approximated simultaneously, as a result the following values of the ϕ meson parameters have been obtained: $m_\phi = 1019.464 \pm 0.060$ MeV/c^2, $\Gamma_\phi = 4.240 \pm 0.017$ MeV, $\frac{B_{\phi\to K^+K^-}}{B_{\phi\to K^0_S K^0_L}} = 1.573 \pm 0.06$ and their accuracy is comparable or better than obtained in previous experiments. We plan to study these processes up to $E_{c.m.} = 2000$ MeV, available with the VEPP-2000 collider.

6 Study of the process $e^+e^- \to K^+K^-\pi^0$

To select events under study the following requirements were applied: two central tracks in DC with two or more photons in the calorimeter. For each pair of photons the kinematics reconstruction was done under assumption that these photons are the product of the π^0 decay. If kinematics of these four particles satisfy energy-momentum conservation and ionization losses in DC correspond to kaons, the combination with the smallest χ^2 is chosen.

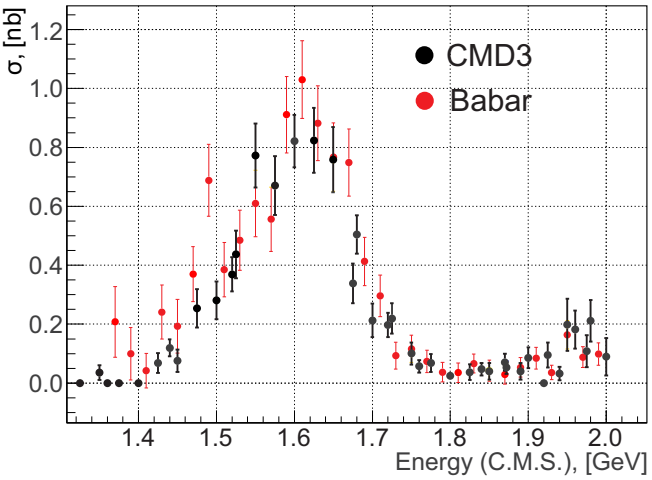

Fig. 7. Preliminary results for $e^+e^- \to K^+K^-\pi^0$ cross section. Black squares — this analysis, red dots — BaBar data. Only statistical errors are shown.

The main physical background comes from the processes $e^+e^- \to \pi^+\pi^-\pi^0$ and $e^+e^- \to \pi^+\pi^-\pi^0\pi^0$ which are significantly suppressed by using dE/dx information. The events of the processes $e^+e^- \to K^+K^-2\pi^0$ and $e^+e^- \to K^+K^-\eta$ are rejected by the kinematics cuts. The detection efficiency was determined with MC simula-

tion, including radiative corrections. Preliminary results of the cross section measurement are shown in Fig. 7 along with BaBar data [11].

7 Study of the process $e^+e^- \to K^+K^-\eta$

The $e^+e^- \to K^+K^-\eta$ process has been earlier studied by the BaBar in the c.m. energy ($E_{\rm c.m.}$) range from 1.56 to 3.48 GeV in the $\eta \to 2\gamma$ decay channel [12], and in the energy range from 1.56 to 2.64 GeV when η decay to $\pi^+\pi^-\pi^0$ [13]. It was found that the main intermediate mechanism is $e^+e^- \to \phi(1680) \to \phi(1020)\eta$, but the statistics was not enough to study the dynamics of the non$-\phi(1020)\eta$ contribution.

The analysis of the $e^+e^- \to K^+K^-\eta$ process is based on an integrated luminosity of 22 pb^{-1} collected in 2011–2012 at 30 c.m. energy points in the range from 1.59 up to 2.0 GeV. The η meson was treated as a recoil particle, and all the modes of η decay were used. To select events under study some cuts were applied: kaons are the product of the $\phi(1020)$ decay, two collinear tracks should be in DC with ionization losses dE/dx which correspond to kaons. The latter condition allows significantly reject physical background.

The distributions in ΔE (defined below) of simulated signal and background events are fitted at every point of energy:

$$\Delta E = E_{K^+} + E_{K^-} + \sqrt{(-\vec{\mathbf{p}}_{K^+} - \vec{\mathbf{p}}_{K^-})^2 + m_\eta^2\}} - 2E_{\rm beam}.$$

For the signal events the fitting function is a sum of three Gaussian functions with the different mean values and widths. The simulated background events are fitted by a second-degree polynomial. The functions found are used to fit the distribution of experimental events in ΔE to determine the number of signal events and was found to be $N_{\rm signal,total} \approx 1454 \pm 48$. The preliminary results of the cross section of $e^+e^- \to \phi(1020)\eta$ process are shown in Fig. 8 along with Babar data.

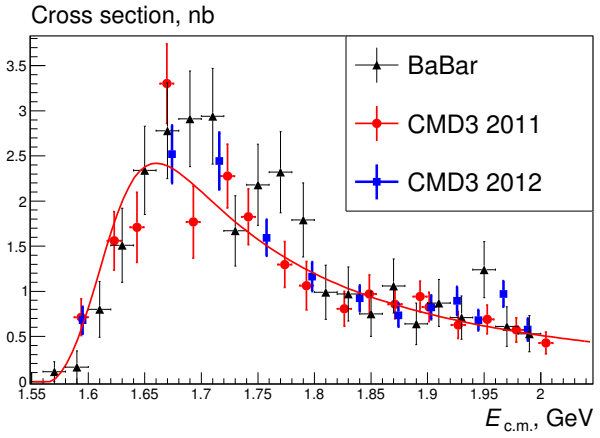

Fig. 8. The cross section of $e^+e^- \to \phi(1020)\eta$ process: CMD-3 results, based on the data collected in 2011 (circular markers) and in 2012 (squared markers) years; BaBar results, measured in $\eta \to 2\gamma$ mode (triangle markers).

8 Study of the processes $e^+e^- \to \eta\gamma$

This process with 3γ in the final state is under study in the whole VEPP-2000 energy range from 400 MeV up to 2 GeV. To select signal events, the following criteria are applied: three or more photons in the calorimeter and no tracks in DC. These three particles should satisfy energy-momentum conservation and the kinematic reconstruction was performed for them. The combination with the smallest χ^2 is used to choose the best group with more than three photons. The number of signal events is determined from a fit of the two-photon invariant mass spectrum. The QED process of e^+e^- annihilation to three photons is the main background and is rejected significantly by kinematics cuts.

The total cross section is calculated according to the formula

$$\sigma(e^+e^- \to P\gamma) = N/[L\,\varepsilon_{NT}\,\varepsilon_{det}\,(1+\delta_{rad})\,B(P \to 2\gamma)],$$

where P stands for π^0 or η, N is the number of signal events, L — integrated luminosity, δ_{rad} — radiation correction, ε_{det} — detection efficiency from Monte Carlo simulation, $B(P \to 2\gamma)$ — branching ratio, and ε_{NT} is a neutral trigger efficiency studied with an $e^+e^- \to e^+e^-\gamma$ process. The preliminary results of the cross section measurement in the energy range around the ϕ meson are presented in Fig 9 with the CMD-2 data [14].

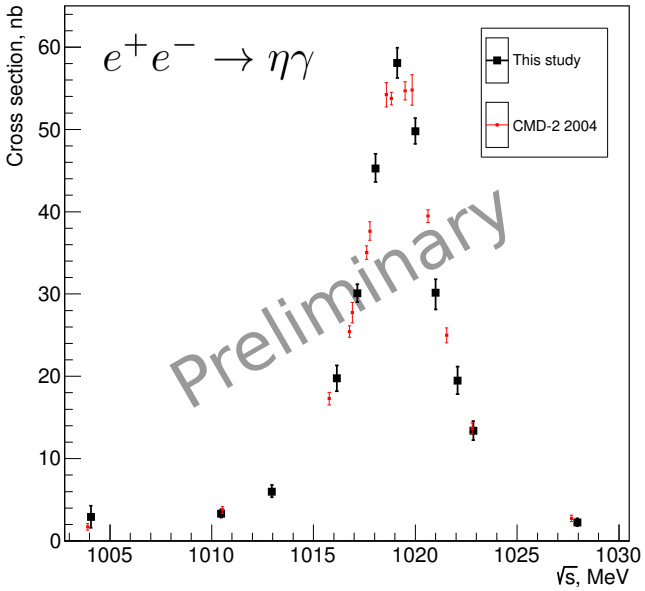

Fig. 9. $e^+e^- \to \eta\gamma$ cross section. Black squares — this analysis, only statistical errors are shown; red dots — CMD-2

9 Study of the process $e^+e^- \to \pi^+\pi^-\pi^0$

The analysis of the process with three pions $\pi^+\pi^-\pi^0$ in the final state was performed using 23 pb^{-1} of data collected in the energy range 1.05 GeV - 1.8 GeV. Events with two reconstructed tracks and at least two detected photons in the barrel calorimeter were selected and then underwent a kinematic reconstruction based on energy-momentum conservation. The combination of two photons which provides the best χ^2 value is selected for a further analysis. Additional cuts on tracks including their recoil mass, momentum, energy losses dE/dx in DC and collinearity are used to suppress the physical background mainly coming from the process $e^+e^- \to \pi^+\pi^-\pi^0\pi^0$. The number of 3π events is obtained by a fit to the two-photon invariant mass distribution using a sum of the signal and background functions. The total number of selected 3π events was found to be 6269. The same procedure has been applied to the sample of Monte-Carlo events which were simulated with a primary generator using the GEANT4 package and then reconstructed with the same software as experimental data. The preliminary results for the Born cross section are shown in Fig. 10 in comparison with the BaBar and SND.

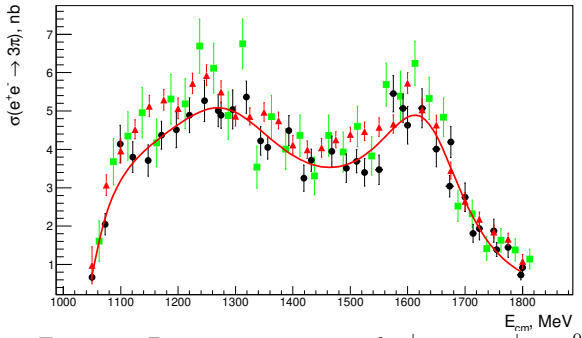

Fig. 10. Born cross section of $e^+e^- \to \pi^+\pi^-\pi^0$. Black points- CMD3, squares - BaBar data, triangles - SND (2015) [15].

10 Study of the process $e^+e^- \to K^+K^-\pi^+\pi^-$

The cross section measurement of the process $e^+e^- \to K^+K^-\pi^+\pi^-$ is based on the integrated luminosity of 22 pb^{-1} in the c.m. energy range from 1.5 to 2.0 GeV and early this process was studied by the BaBar via ISR [16]. Nevertheless. The direct measurements are very important, since some contributions to a_μ are based on isospin relations of various $K\bar{K}n\pi$ final states. Any uncertainty of this approach will be crucial for a_μ accuracy.

The signal events should have three or four tracks in DC coming from the interaction region and obey the energy-momentum conservation. Two tracks corresponding to kaons should have the large ionization losses dE/dx in DC and this information was input to a likelihood function constructed for further K/π separation. Figure 11 shows a scatter plot of the difference between the measured total energy and c.m. energy $\Delta E_4 = E_{tot} - E_{c.m.}$ vs the total momentum for all events with four tracks.

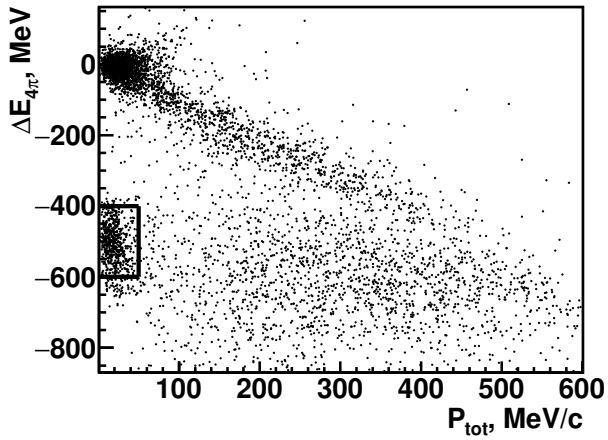

Fig. 11. Scatter plot of the difference between the total energy and c.m. energy (ΔE_4)versus the total momentum for four-track events. The upper cluster of dots represents $\pi^+\pi^-\pi^+\pi^-$ while the lower one - $K^+K^-\pi^+\pi^-$ events.

The cluster of $\pi^+\pi^-\pi^+\pi^-$ events is located near the origin of coordinates. The cluster of signal events with a zero total momentum is shifted down along the vertical axis.

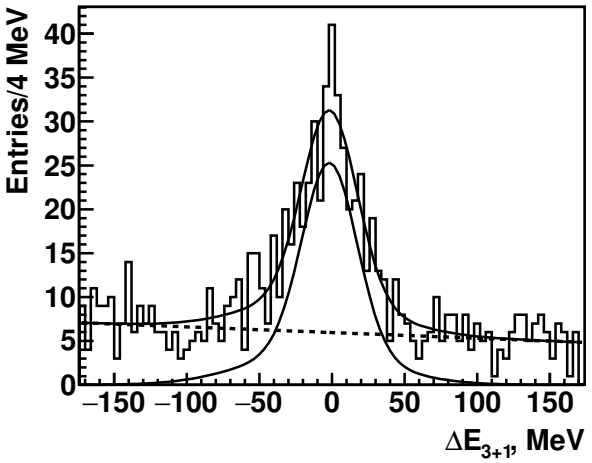

Fig. 12. The histogram of the difference between the calculated total energy with energy of fourth particle ΔE_{3+1} and c.m. energy. Upper smooth line - histogram fit, dotted line - background fit, lower smooth curve - fit simulated signal events.

A similar procedure was used to select signal events with three tracks in DC. For these events energy deficit should

correlate with the total (missing) momentum. For such events, the energy of a missing particle is calculated and added to the energy of three detected particles. The difference between the obtained energy ΔE_{3+1} and c.m. energy is shown in Fig. 12. The signal events are clearly seen. To obtain the number of $K^+K^-\pi^+\pi^-$ events the histogram was fitted with a sum of two Gaussian distributions for a signal peak and a quadratic polynomial for background. As a result, ∼13300 four-track events and ∼16000 three-track events were selected. To obtain a detection efficiency, the $K^+K^-\pi^+\pi^-$ events were simulated with a primary generator using the GEANT4 package and then reconstructed with the same software as experimental data.

Production mechanisms with the $K^+K^-\rho$, $K1(1270,1400)K \to K^*\pi K$, $\phi\pi^+\pi^-$ and K^*K^* intermediate states are required to correctly describe angular and invariant mass distributions of the experimental data and to determine the detection efficiency which was found to be ∼50-60%.

The cross section as a function of energy, shown in Fig. 13, and well agrees with the previous BaBar measurement [17] presented by open circles. Systematic error is under study and currently is estimated as 6%. The main systematic uncertainty is due to the theoretical model, describing intermediate states, affects the detection efficiency.

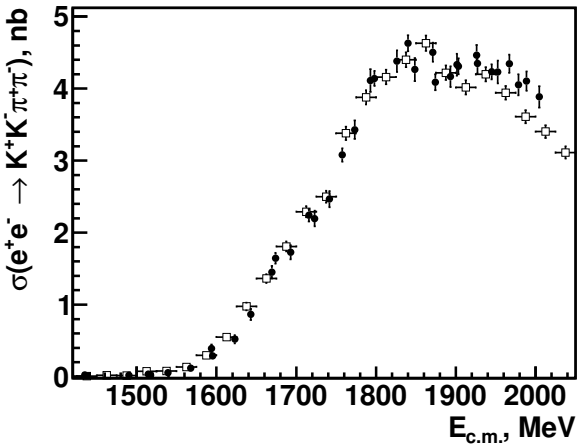

Fig. 13. Dots - the $e^+e^- \to K^+K^-\pi^+\pi^-$ cross section measured with the CMD-3 detector. The BaBar results are shown by open circles.

11 Production of six pions

Production of six pions in e^+e^- annihilation was studied at DM2 [18] and BaBar [19]. The DM2 experiment observed a "dip" in the cross section of the process $3(\pi^+\pi^-)$ near 1.9 GeV, confirmed later by the BaBar. The origin of the "dip" remains unclear, but the most popular explanation is related to opening $p\bar{p}$ and $n\bar{n}$ channels discussed in many theoretical papers [20].

The analysis is based on 22 pb^{-1} of integrated luminosity collected in the c.m. energy range from 1.5 to 2 GeV. Candidates for the process under study are required to have five or six tracks in DC. For six- or five-track candidates the total energy and total momentum are calculated, assuming all tracks to be pions:

$$\mathrm{Etot} = \sum_{i=1}^{5,6} \sqrt{\mathrm{p_i^2 + m_\pi^2}}\ , \qquad \mathrm{Ptot} = |\sum_{i=1}^{5,6} \bar{\mathrm{p}}_i|.$$

Figure 14 shows a scatter plot of the difference between the total energy and c.m. energy $\Delta \mathrm{E}_6 = \mathrm{E}_{tot} - \mathrm{E}_{c.m.}$ versus momentum for six-track candidates. A clear signal of six-pion events is seen as a cluster of dots near zero and "tail" which corresponds to events when initial electrons (positrons) radiate photons. The events with total momentum less than 150 MeV/c and with the difference $\Delta \mathrm{E}_6$, -200< $\Delta \mathrm{E}_6$ <100 MeV, are required to determine the number of six-pion events. To estimate the background MC simulation of the major processes $2(\pi^+\pi^-\pi^0)$ and $2(\pi^+\pi^-)\pi^0$ was performed and was found to be smaller than 1%.

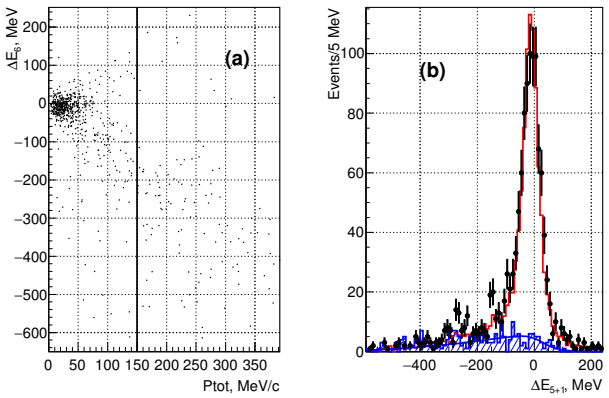

Fig. 14. (a) A scatter plot of the difference between the total energy and c.m. energy (ΔE_6) versus total momentum for six-track events. The vertical line shows the applied selection.(b) The number of events is shown in the right plot. Points with errors are data, the histogram represents the MC simulated events. The shaded histogram shows an estimate of background events with a fit function used to subtract background.

To determine the number of events with one missing particle, a sample with five selected tracks is used. These events have energy deficit correlated with the total (missing) momentum. The energy of a missing particle is calculated and added to the energy of five detected pions. The difference of the obtained energy and c.m. energy $\Delta \mathrm{E}_{5+1}$ is shown in the left part of the same

graph by points together with the simulated background mainly coming from the processes $e^+e^- \to 2(\pi^+\pi^-\pi^0)$ and $e^+e^- \to 2(\pi^+\pi^-)\pi^0$ and shown by a solid line.

The polynomial fit parameters vary for the experimental and MC simulated background distributions as well as different cuts that lead to a ∼3% uncertainty in the number of signal events. A more detailed analysis can be found in [21]. We have studied intermediate states in the final state with six charged pions and came to the following conclusion: the dynamics production changes versus energy and this phenomenon demands a further investigation. High statistics, which will be obtained at VEPP-2000, will allow to study dynamics with much better accuracy and reduce the models systematics. Calculation results for the cross section are presented in Fig 15

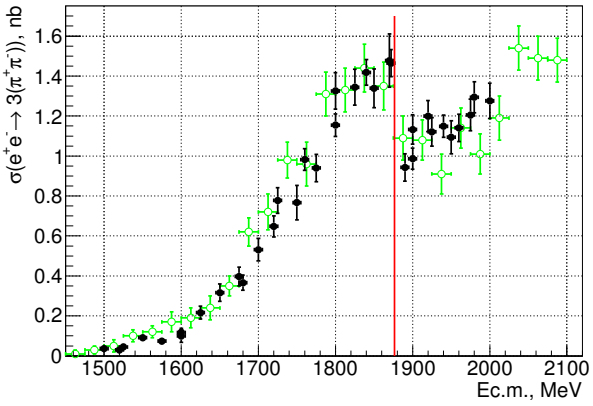

Fig. 15. Measurement of the $e^+e^- \to 3(\pi^+\pi^-)$ cross section with the CMD-3 - black points, BaBar data - open circles.

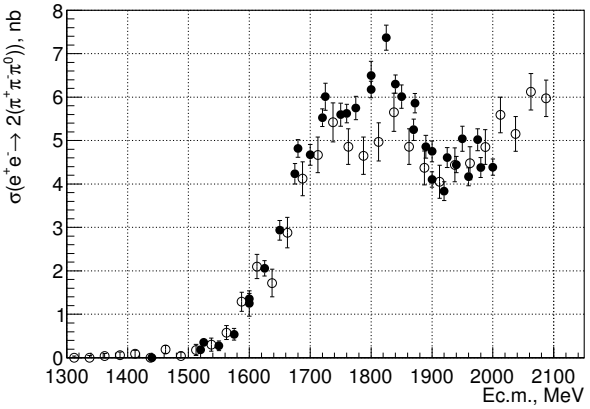

Fig. 16. Measurement of the $e^+e^- \to 2(\pi^+\pi^-\pi^0)$ cross section at CMD-3 - black points, open circles - BaBar data.

To measure the cross section of the process $e^+e^- \to 2(\pi^+\pi^-\pi^0)$ a sample of events with four charged and two neutral pions was selected. To select neutral pions, the spectrum of invariant mass of all two-photon combinations was studied inside the energy gap from $60 < m_{\gamma\gamma} < 200$ MeV/c^2 and a combination with the nearest to the pion mass is chosen.

The number of signal events at each energy point was determined by a fit of the ΔE distribution, which represents the difference between the total energy of event $e^+e^- \to 2(\pi^+\pi^-\pi^0)$ and c.m. energy $E_{c.m.}$: $\Delta E = E(2(\pi^+\pi^-\pi^0)) - E_{c.m.}$. A sum of three Gaussian functions for signal events and quadratic polynomial for background were used to describe this doistribution. The cross section is calculated according to the number of determined events and takes into account radiative corrections and detection efficiency. The results for the cross section are presented in Fig. 16. The analysis of the data is going on now.

12 Cross sections measurement of the $e^+e^- \to \eta\pi^+\pi^-$ and $e^+e^- \to \omega\pi^+\pi^-$ processes

12.1 $e^+e^- \to \eta\pi^+\pi^-$, $\eta \to \gamma\gamma$

The candidates for events under study with two tracks in DC and two or more photons were selected. A combination of two photons with the best χ^2 is chosen and events of $\gamma\gamma\pi^+\pi^-$ undergo a kinematic fit. To calculate the number of the $\eta\pi^+\pi^-$ events the invariant mass distribution is fitted and shown in Fig. 17, a at the energy point 1500 MeV.

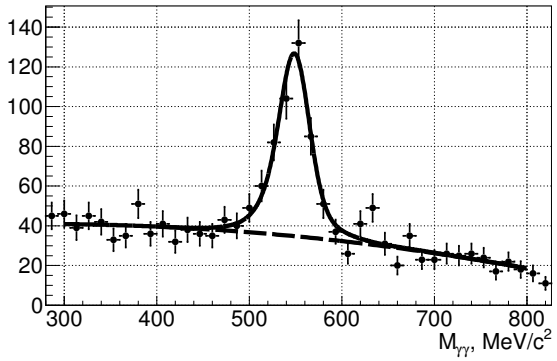

Fig. 17. The fit of two-photon invariant mass at the energy of 1500 MeV shown with a linear fit for the background.

The preliminary results for the cross section of the $e^+e^- \to \eta\pi^+\pi^-$ process are plotted in Fig. 18 with SND results [22]. The systematic uncertainty for this process is about 5.2% and mainly due to the detection efficiency, which one depends on the theoretical model describing the angular distribution of the final particles and was calculated using Monte Carlo simulation. Two different fits

of the $e^+e^- \to \eta\pi^+\pi^-$ Born cross section under the VDM model are presented too with/without $\rho(1700)$. At the current statistics it is not possible to make a conclusion about presence of the $\rho(1700)$.

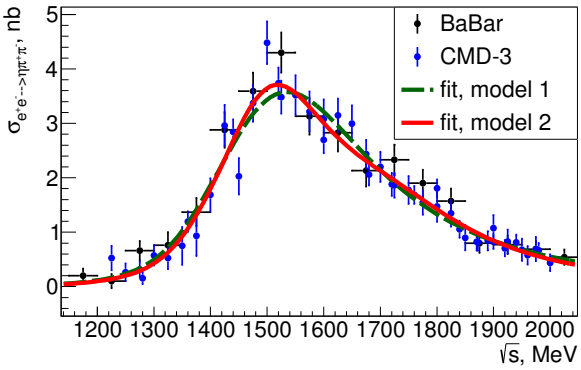

Fig. 18. The $e^+e^- \to \eta\pi^+\pi^-$ Born cross section measured in the $\eta \to \gamma\gamma$ channel. The results are presented together with BaBar data.

12.2 $e^+e^- \to \eta\pi^+\pi^- \to \pi^+\pi^-\pi^0\pi^+\pi^-$, $e^+e^- \to \omega\pi^+\pi^- \to \pi^+\pi^-\pi^0\pi^+\pi^-$

The form of the $\pi^+\pi^-\pi^0$ invariant mass distribution for the $e^+e^- \to \pi^+\pi^-\pi^+\pi^-\pi^0$ process has been determined with Monte Carlo simulation and was used to determine the numbers of the signal events under study. The preliminary results for the Born cross sections of the $e^+e^- \to \eta\pi^+\pi^-$ and $e^+e^- \to \omega\pi^+\pi^-$ processes are shown in Fig. 19 and 20.

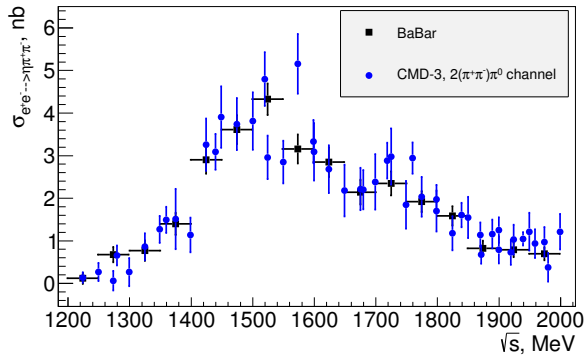

Fig. 19. The $e^+e^- \to \eta\pi^+\pi^-$ Born cross sections measured when η decay into three pions $\pi^+\pi^-\pi^0$. The results are presented together with BaBar data.

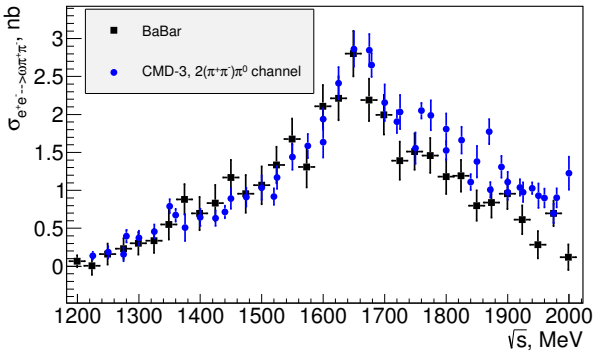

Fig. 20. The $e^+e^- \to \omega\pi^+\pi^-$ Born cross sections measured when ω decays into three pions $\pi^+\pi^-\pi^0$. The results are presented together with BaBar data.

The current systematic uncertainty for these channels is estimated as 15%.

13 Study of the process $\omega \to \pi^0 e^+ e^-$

This process was earlier studied with the CMD-2 detector [23]. The current analysis is based on an integrated luminosity of 10 pb^{-1} collected in the center-of-mass energy range 760÷840 MeV. The ω decay to $\pi^0 e^+ e^-$ has been studied using the π^0 dominant decay mode: $\pi^0 \to \gamma\gamma$. The main background for this process comes from the decay ω to $\pi^+\pi^-\pi^0$ and to $\pi^0\gamma$ followed by the Dalitz decay of the π^0 or γ conversion in the material in front of the drift chamber and QED processes. To select signal events under study, different cuts were applied. In particular, to suppress events from decay $\omega \to \pi^+\pi^-\pi^0$ the following parameters were used: an opening angle between tracks should be $\Delta\psi \leq 1$ rad, the spectra of the recoil mass of photon pairs and some features of the kinematic decay. The separation method for $\pi^0 e^+ e^-$ and $\pi^0\gamma$ (with γ conversion on the material in front of DC) is based on the information about momentum of the track and vertex position which uses a neural network. The efficiency of suppression is: for $\pi^0\gamma \sim 84\%$, while we lose $\sim 2\%$ of signal events.

The detection efficiency $\epsilon_{\pi^0 e^+ e^-} = 22\%$ was determined using MC simulation based on the GEANT4 package. The number of signal events has been obtained from a fit of the $\gamma\gamma$ invariant mass distribution at each energy point. These values were used to determine the visible cross section shown in Fig. 21.

The total number of selected $\omega \to \pi^0 e^+ e^-$ events is 1228. The current value of $B(\omega \to \pi^0 e^+ e^-) = (7.15 \pm 0.38)10^{-4}$, where the trigger efficiency, efficiency of reconstruction of close tracks and the contributions come from $\omega \to \pi^+\pi^-\pi^0; \omega \to \pi^0\gamma$ were not taken into account. The analysis is still in progress.

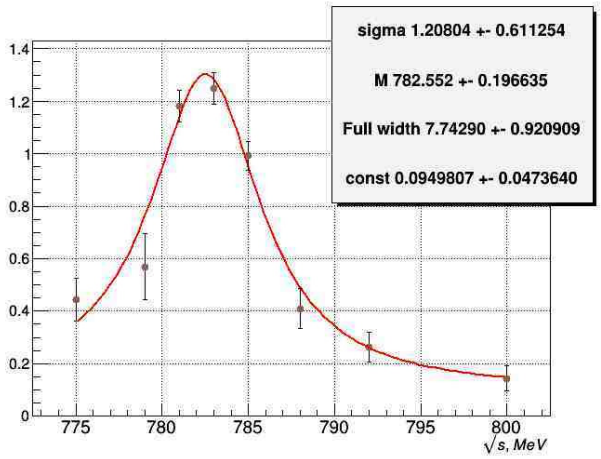

Fig. 21. The visible cross section for the process $\omega \to \pi^0 e^+ e^-$.

14 Summary and conclusion

VEPP-2000 successfully operates with a goal to get ~ 1 fb^{-1} in 5-10 years and provide new precise results on the hadron production. The current integrated luminosity was measured using two well-known QED processes $e^+e^- \to e^+e^-$, $\gamma\gamma$. Two types of the first level triggers "CHARGED" and "NEUTRAL" delivered the independent information that allowed to determine the detection efficiencies and to estimate their uncertainties. Data analysis is in progress, the already collected data sample delivers the same or better statistical precision for the hadronic cross sections than in previous experiments.

Acknowledgements

The authors are grateful to A.I. Milstein for the help with a theoretical interpretation and development of the models. We thank the VEPP-2000 team for excellent machine operation.

This work is supported in part by the Russian Education and Science Ministry, by FEDERAL TARGET PROGRAM "Scientific and scientific-pedagogical personnel of innovative Russia in 2009-2013", by agreement 14.B37.21.07777, by the Russian Fund for Basic Research grants RFBR 10-02-00695-a, RFBR 10-02-00253-a, RFBR 11-02-00328-a, RFBR 11-02-00112-a, RFBR 12-02-31501-mol-a, RFBR 12-02-31499-mol-a, RFBR 12-02-31498-mol-a, RFBR 12-02-01032-a, RFBR 13-02-00215-a, RFBR 15-02-05674-a.

References

1 I.A.Koop *et al.*, Nucl.Phys.B, Proc.Suppl. **181**, 371 (2008).
2 B.I.Khazin *et al.*, Nucl.Phys.B, Proc. Suppl. **181-182**, 376 (2008).
3 M.N.Achasov *et al.*, Nucl.Instrum.Meth. **A598**, 31 (2009).
4 M.Davier *et al.*, EPJ **C31**, 503 (2003).
5 G.Grawford *et al.*, NIM **A345**, 429 (1994).
6 E.V.Abakumova *et al.*, Phys.Rev.Lett. **110**, 140402 (2013).
7 R.R.Akhmetshin *et al.*, JINST **9** (2014) C09003.
8 A.B.Arbuzov *et al.*, EPJ **C46**, 689 (2006).
9 I.B.Logashenko *et al.*, 2014. EPJ Web Conf. 72 (2014) 00013.
10 E.A. Kozyrev *et al.*, Phys.Atom.Nucl. 78 (2015) 3, 358-362, Yad.Fiz. 78 (2015) 5, 388-392;
R.R. Akhmetshin *et al.*, Phys.Lett. B **695**, 412 (2011);
J. P. Lees *et al.*, Phys. Rev. D **88**, 032013 (2013).
11 B.Aubert *et al.*, Phys. Rev. D **77**, 092002 (2008).
12 B.Aubert *et al.*, Phys. Rev. D **76**, 092005 (2007).
13 B.Aubert *et al.*, Phys. Rev. D **77**, 092002 (2008).
14 R.R.Akhmetshin *et al.*, Phys. Lett., B **605** 36 (2005).
15 V.M.Aulchenko *et al.*, Phys. Rev. D **91**, 052013 (2015);
B.Aubert *et al.*, Phys.Rev. D 70 (2004) 072004.
16 B.Aubert *et al.*, Phys. Rev. **D77**, 092002 (2008).
17 J.P.Lees *et al.*, Phys. Rev. **D85**, 012008 (2012).
18 R.Baldini *et al.*, reported at the "Fenice" Workshop, Frascati (1988);
A.B.Clegg and A. Donnachie, Z. Phys. C**45**, 677 (1990);
M.R.Whalley, J. Phys. G**29**, A1 (2003).
19 B.Aubert *et al.,* Phys. Rev. D**73**, 052003 (2006).
20 A.Sibirtsev and J. Haidenbauer, Phys. Rev.D **71**, 054010 (2005).
21 R.R.Akhmetshin *et al.*, Phys.Lett. B **723**, 82 (2013).
22 V.M.Aulchenko *et al.*, Phys. Rev. D **91**, 052013 (2015);
B.Aubert, *et al.*, Phys. Rev. D. **76**, 092005 (2007).
23 R.R.Akhmetshin *et al.*, Phys.Lett. B613 **29-38**, (2005).